Structure and Magnetism of Neutral and Anionic Palladium Clusters

M. Moseler, H. Häkkinen, R. N. Barnett, and Uzi Landman
School of Physics, Georgia Institute of Technology, Atlanta, Georgia 30332-0430
(Received 15 August 2000)

The properties of neutral and anionic Pd_N clusters were investigated with spin-density-functional calculations. The ground-state structures are three dimensional for $N > 3$ and they are magnetic with a spin triplet for $2 \leq N \leq 7$ and a spin nonet for $N = 13$ neutral clusters. Structural and spin isomers were determined and an anomalous increase of the magnetic moment with temperature is predicted for a Pd_7 ensemble. Vertical electron detachment and ionization energies were calculated and the former agrees well with measured values for Pd_N^-.

DOI: 10.1103/PhysRevLett.86.2545 PACS numbers: 36.40.Cg, 36.40.Mr, 36.40.Wa, 61.46.+w

Enhancement of magnetism in clusters of elements that are ferromagnetic as bulk solids has been demonstrated through Stern-Gerlach (SG) deflection measurements [1], and it is understood to derive from reduced atomic coordination resulting in stronger electron localization. However, the emergence of magnetism in small clusters of close-shell nonmagnetic atoms is clouded by uncertainty. Palladium aggregates (with a [Kr] $4d^{10}$ atomic structure) are particularly interesting since the bulk metal is known to be "almost" magnetic, with the emergence of magnetism predicted to require a mere 6% lattice expansion [2]. Experimental information is limited to SG measurements on Pd_N clusters with $N > 12$ (which were found to be nonmagnetic) [3] or to inferences from (nonmagnetic) photoemission studies [4]. Systematic theoretical investigations of magnetic properties are lacking, limited only to neutral Pd_{13} [5,6].

We report on an extensive density-functional-theory study pertaining to size-dependent patterns of the properties of Pd_N and Pd_N^- clusters with $N = 1-7$ and $N = 13$. The ground states (GSs) of the neutral and anionic clusters are found to undergo an early transition (i.e., for $N > 3$) to three-dimensional (3D) ones and possess a nonzero magnetic moment. In addition to higher-energy structural isomers (STIs) we determined sequences of close-lying spin isomers (SPIs). For a Pd_7 ensemble, we predict an increase of the magnetic moment with temperature due to the thermal accessibility of such isomers. All the SPIs exhibit high local magnetic moments (LMMs), including the singlet states with an antiferromagnetic LMM coupling. Our structural determinations are corroborated by the remarkable agreement between the calculated vertical electron detachment energies (vDEs) from the cluster anions and photoelectron spectroscopy (PES) measurements [4,7,8].

In this study the Kohn-Sham (KS) equations with generalized gradient corrections [9] were solved using the Born-Oppenheimer local-spin-density molecular dynamics method [10], with scalar-relativistic [11] nonlocal pseudopotentials [12]. Cluster geometries were determined via symmetry-unrestricted structural optimizations through an exhaustive search among various structures including those suggested for certain Pd clusters [13–15] and other metal clusters [16,17]. For each structure spin-restricted optimizations were performed covering all energetically important spin multiplicities.

The GS geometries and STIs for both Pd_N and Pd_N^- are rather similar and they follow the same structural evolution, exhibiting Jahn-Teller distortions from the ideal symmetric structures (see Fig. 1), with a transition to 3D configurations at $N > 3$ [18]. The GSs (i.e., maximal binding energy E_B in Fig. 1) of Pd_N with $N \leq 7$ have a triplet ($S = 1$) spin multiplicity (see open squares in Figs. 1A–1F), while for Pd_{13} the GS is associated with a nonet ($S = 4$) spin configuration (see Fig. 1G). On the other hand, the GS spin multiplicities of the Pd_N^- anions (filled symbols in Fig. 1) vary nonmonotonically with N (doublet for $N = 2$, 3, 4, and 6; quartet for $N = 5$; sextet for $N = 7$, and octet for $N = 13$). We note here that the higher-lying STIs [19] and SPIs of the neutral and anionic clusters become thermally accessible with increasing cluster size (see temperature scales [20] on the right-hand side of Fig. 1).

The binding energies of the GS clusters increase rather monotonically with N (Fig. 2a), showing enhanced local stabilities for Pd_3^- and Pd_4 [21]. The average nearest-neighbor bond lengths ($\langle R_{nn} \rangle$) of the GS structures and the SPIs are very similar [22], converging rapidly to the bulk value (2.75 Å [23]).

The calculated vDEs from the cluster anions are in remarkable agreement with values determined from PES measurements [4,7,8] (Fig. 2b). For all the clusters, we display the vDEs only for the GS (structural and spin) configurations of the anions, except for Pd_7^- where we show the vDEs for both the GS ($S = 5/2$) and its next (higher-in-energy) SPI ($S = 3/2$) (the difference in energy between the two isomers is 0.11 eV, corresponding to only 170 K in vibrational temperature [20]), with the latter exhibiting a better agreement with the experimental data. These results suggest that for Pd_7^- the measured vDE may correspond to this higher-energy SPI which is accessible already at very low temperatures, while for the other clusters studied here the vDEs are determined by the GS structures over a broad temperature range.

The only (slight) discrepancy between the calculated and measured vDEs is for Pd_3^- (see Fig. 2b). However, we observe from this figure that the predicted vDE (2.0 eV) for Pd_3^- is rather close to the dissociation energy (E_D) of the process $Pd_3^- \rightarrow Pd_2^- + Pd$ (see filled circle in Fig. 2b at $E_D = 2.41$ eV, compared to a measured value of 2.26 eV [24]). This implies that this dissociation channel may compete with the electron detachment under appropriate experimental conditions. Consequently, we assign the vDE of Pd_3^- to the next higher feature in the measured PES [8]) occurring at 1.88 eV which agrees with the predicted value, and the lower measured value (at 1.66 eV, marked by a cross in Fig. 2b) is attributed to the vDE of a (hot) Pd_2^- dissociation product [25] (the same conclusions apply to the photoelectron spectrum of Pd_3^- shown in Fig. 2 of Ref. [4]); for a similar interpretation of the measured PES of Au_3^-, see Refs. [16] and [26].

The vertical ionization potentials predicted by us (vIP in Fig. 2c) start at the atomic value of 8.28 eV compared to the measured first IP of Pd, 8.33 eV [23]; the calculated second IP of Pd (27.34 eV) also agrees with the experimental one (27.75 eV) [23]. The predicted values for $N = 2$ and 3 are close to each other followed by a marked drop for clusters with $N > 3$, which is likely to reflect the transition to 3D structures. Convergence to the bulk limit (the work function of Pd is 4.97 eV [27]) is slow. No measured IP values have been reported.

The multitude of spin multiplicities for the Pd_N^- clusters results in a considerable variation of the magnetic moment per atom $\mu = 2S\mu_B/N$ (solid squares in Fig. 2d) with particularly high values of $\mu = 0.6$, 0.71, and $0.54\mu_B$ for $N = 5$, 7, and 13, respectively. On the other hand, the occurrence of a triplet GS for the neutral clusters underlies a monotonic $1/N$ decrease of μ for $N = 1-7$ (open squares in Fig. 2d), with an unexpected high value of $0.62\mu_B$ for Pd_{13} which is higher than the experimental [3] estimate ($\mu < 0.4\mu_B$).

The rather surprising existence of energetically favorable high-spin isomers for Pd clusters originates from *sd* hybridization developing upon bonding, with the *d*-orbitals' weight diminished somewhat on each atom, resulting in a situation reminiscent of open-shell transition metals. The total magnetic moment of the cluster is comprised of sizable atomic LMMs [$\mu_\ell \sim \pm(0.3 - 0.6)\mu_B$] that couple antiferromagnetically in the spin-compensated

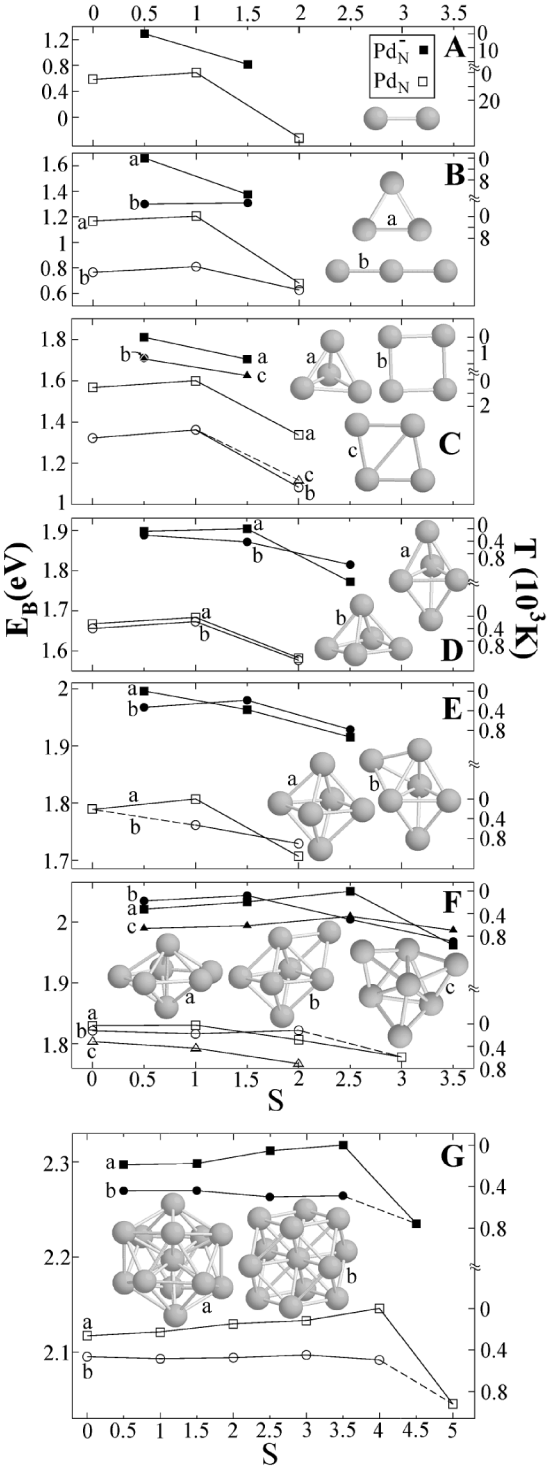

FIG. 1. Binding energies E_B (in eV) of structural (a, b, c) and spin ($S = 0$, 1/2, 1, 3/2, etc.) isomers of Pd_N^- and Pd_N for $N = 1-7$ (A)–(F) and 13 (G). Filled and open symbols represent anions and neutrals, respectively, and squares for the ground-state structure (a), circles for structures (b), and triangles for (c). The anionic E_B is defined as the energy per atom to separate Pd_N^- into N neutral atoms and an electron. The E_B values on the left-hand side of the panels are mapped on separate temperature scales [20] (T, in K) for the anions (top values on the right-hand axis of each panel) and the neutrals (bottom values), giving an estimate of the thermal accessibility of the isomers. Note the large number of isomers for Pd_7 and Pd_7^- for $T < 400$ K. Some of the structural isomers were not stable for certain spin values (such cases are denoted by dashed lines). The Pd_4^- square (b) in panel (C) transformed into a rhombus (c) for $S = 3/2$ and the Pd_4 rhombus transformed into a square for $S = 0$ and 1. The Pd_6 capped trigonal bipyramid (b) transformed to the octahedron (a) for $S = 0$. The Pd_7 capped octahedron (b) became a pentagonal bipyramid (a) for $S = 3$ and the Pd_{13} and Pd_{13}^- cuboctahedron (b) transformed to the icosahedron (a) for $S = 9/2$ and 5, respectively.

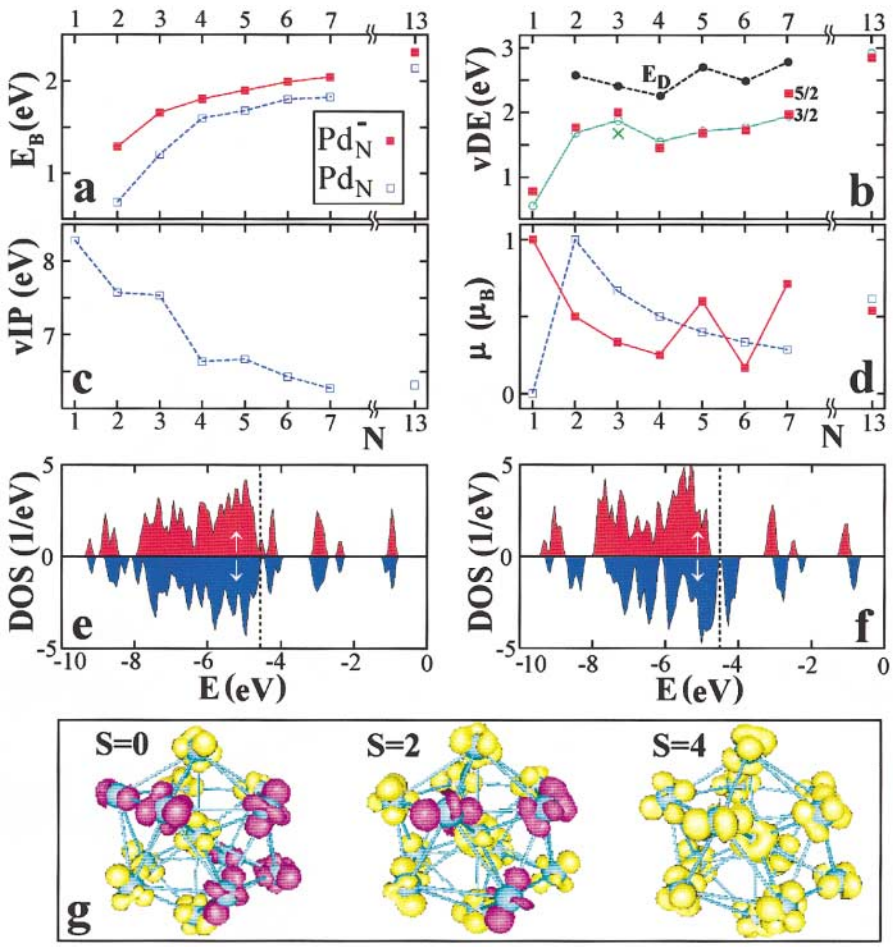

FIG. 2 (color). Size evolution [panels (a)–(d)] of energetic and magnetic quantities in Pd clusters. (a) Binding energy per atom, E_B (in eV); (b) theoretical (filled squares) and experimental (open circles) vertical electron detachment energy (vDE) and the calculated atom dissociation energy E_D of the anions (filled circles). Experimental values are taken from Refs. [7,8] for $N = 1-3$ (the corresponding results shown for Pd_3^- in Fig. 2 of Ref. [4] are essentially the same) and from [4] for $N = 4-7$ and 13. The cross and the open circle at $N = 3$ correspond to the maximum of peak A and the peak of group B–H in Fig. 1 of Ref. [8], respectively (and correspondingly for the first and second peaks in Fig. 2 of Ref. [4]). For Pd_7^-, we show the vDE of the GS ($S = 5/2$) and a thermally accessible SPI ($S = 3/2$). The vDE of Pd_1^- was estimated according to Janak's theorem [28] by the highest occupied molecular orbital energy of $Pd_1^{-1/2}$; (c) calculated vertical ionization potentials; (d) the magnetic moment per atom of the GS anions (filled squares) and of the GS neutrals (open squares). (e),(f) Density of states (DOS, in 1/eV) of singlet (e) and nonet (f) icosahedral Pd_{13} clusters. (g) Constant-value images of spin-polarization density in singlet, quintet, and nonet icosahedral Pd_{13} (left, middle, right, respectively) clusters. The purple and yellow denote excess of minority and majority spins, respectively. Note the transition from antiferromagnetic to ferromagnetic ordering when going from the singlet to the nonet.

singlet states, and align themselves in SPIs with high total μ. This is illustrated for the icosahedral Pd_{13} cluster in Fig. 2 where the (gapless) density of states (DOS) of the $S = 0$ singlet SPI is shown in Fig. 2e and the corresponding spin-polarization density in Fig. 2g (left); note the nonuniform spatial distribution of the spin polarization reflected in the different line shapes of the DOS of the up and down spins. In the $S = 2$ spin-quintet SPI the minority spin polarization is localized on three sites located in a triangle (Fig. 2g, middle). In the $S = 4$ spin-nonet GS cluster all the sites are spin polarized in the same direction (Fig. 2g, right), and its stability is reflected in the large gap in the majority-spin DOS near the Fermi energy (see spin ↑ in Fig. 2f).

Intriguing conclusions can be made regarding the thermal behavior of certain Pd clusters in SG measurements; here we consider the case of Pd_7 and Pd_7^- at room temperature. Neglecting the vibrational and entropic differences between the isomers, the probability to find a cluster with spin S, irrespective of its atomic isomeric structure, is given by $P_{N,T}(S) = \sum_I \exp(\frac{NE_B(N,I,S)}{k_B T})/Z_{N,T}$ with the Boltzmann constant k_B, the ensemble temperature T, the structural isomer index I, and the (normalizing) partition function $Z_{N,T}$. Several spin isomers of the neutral as well as the anionic heptamer have a finite $P_{7,T}(S)$ (Fig. 3a) even for low temperatures, leading us to predict that in a SG experiment up to three different deflection angles should be measurable. Note that while an increase in temperature depopulates the Pd_7 pentagonal bipyramid triplet ($S = 1$) GS, the singlet ($S = 0$) state of that structure and the capped octahedron quintet ($S = 2$) state (Fig. 1F) gain statistical weight. Consequently, we predict that for Pd_7 a rise in temperature would lead first to a decrease of the thermally averaged magnetic moment per atom $\langle\mu\rangle_{N,T} = \sum_S 2S\mu_B P_{N,T}(S)/N$ due to a sharp increase in the population of the singlet state. The subsequent increase of $\langle\mu\rangle_{N,T}$ (see Fig. 3b, $T > 200$ K) results from the higher thermal population of the quintet state relative to the GS triplet (Fig. 3a) [29]. Such anomaly does not occur in the case of the Pd_7^- cluster where the doublet ($S = 1/2$) and quartet ($S = 3/2$) states start to coexist with the sextet ($S = 5/2$) GS at elevated temperatures (Fig. 3a). For both neutral and anionic Pd_{13}, the higher-lying isomers play essentially no role for $T < 800$ K resulting in a weak temperature dependence of $\langle\mu\rangle_{N,T}$ (Fig. 3b).

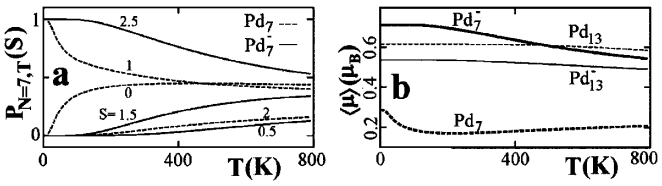

FIG. 3. (a) Population probabilities of the different SPIs (irrespective of the structure) of neutral (dashed curves) and anionic (solid curves) heptamers; (b) thermally averaged magnetic moments per atom for Pd_7, Pd_7^-, Pd_{13}, and Pd_{13}^-.

In summary, we found that unlike atomic and bulk Pd, both neutral and anionic Pd_N clusters ($2 \leq N \leq 7$ and $N = 13$) are magnetic, with relatively high LMMs. Underlying this behavior is the hybridization of atomic *s* and *d* states when clusters are formed that depletes local *d* contribution around each atom and leads to an open-shell-like behavior. The abundance of close-lying SPIs for certain clusters should be detectable in thermally controlled SG experiments, and we predict an ensemble of Pd_7 clusters to exhibit an (anomalous) increase of the magnetic moment with temperature. The remarkable agreement between the calculated and measured vDEs of the cluster anions corroborates the predicted atomic structures. Our results provide the first quantitative predictions pertaining to the emergence of pronounced magnetic properties of Pd_N and Pd_N^- clusters, unlike the weak magnetic tendencies inferred indirectly from PES data [4]; note, in particular, the contrast between our results for Pd_7 (see Fig. 2d and Fig. 3) and the suggestion of a zero spin GS for Pd_7 given in Ref. [4]. Furthermore, our study motivates temperature-dependent magnetic deflection (SG) measurements and further investigations of free and supported Pd clusters, including correlations between their magnetic properties and their catalytic activity [30].

This work is supported by the U.S. DOE, the Deutsche Forschungsgemeinschaft (M. M.), and the Academy of Finland (H. H.). Computations have been done on IBM SP2 at the Georgia Tech Center for Computational Materials Science and on Cray T3E at NERSC.

[1] I. M. L. Billas *et al.,* Science **265**, 1692 (1994).
[2] V. L. Moruzzi and P. M. Marcus, Phys. Rev. B **39**, 471 (1989).
[3] A. J. Cox *et al.,* Phys. Rev. B **49**, 12 295 (1994).
[4] G. Ganteför and W. Eberhardt, Phys. Rev. Lett. **76**, 4975 (1996).
[5] B. V. Reddy *et al.,* Phys. Rev. Lett. **70**, 3323 (1993).
[6] N. Watari and S. Ohnishi, Phys. Rev. B **58**, 1665 (1998).
[7] J. Ho *et al.,* J. Phys. Chem. **95**, 4845 (1991).
[8] K. M. Ervin *et al.,* J. Phys. Chem. **89**, 4514 (1988).
[9] J. P. Perdew *et al.,* Phys. Rev. Lett. **77**, 3865 (1996).
[10] R. Barnett and U. Landman, Phys. Rev. B **48**, 2081 (1993).
[11] L. Kleinman, Phys. Rev. B **21**, 2630 (1980); G. B. Bachelet and M. Schlüter, Phys. Rev. B **25**, 2103 (1982).
[12] N. Troullier and J. L. Martins, Phys. Rev. B **43**, 1993 (1991). The core radii (in units of a_0) are $s(2.45)$, $p(2.6)$, and $d(2.45)$ with *s* as the local component. A plane-wave basis with a 61.67 Ry cutoff was used.
[13] D. Dai and K. Balasubramanian, Chem. Phys. Lett. **310**, 303 (1999), and references therein.
[14] G. Valerio and H. Toulhoat, J. Phys. Chem. **100**, 10 827 (1996).
[15] K. M. Neyman *et al.,* Appl. Catal. **191**, 3 (2000).
[16] H. Häkkinen and U. Landman, Phys. Rev. B **62**, R2287 (2000).
[17] V. Bonacic-Koutecky *et al.,* J. Chem. Phys. **98**, 7981 (1993).
[18] The symmetries of the ideal structures are Pd_3: D_{3h} equilateral triangle, Pd_4: T_d tetrahedron, Pd_5: D_{3h} trigonal bipyramid, Pd_6: O_h octahedron, Pd_7: D_{5h} pentagonal bipyramid, and Pd_{13}: I_h icosahedron. Atomic coordinates of the neutral and anionic clusters are available upon request.
[19] The ideal symmetries of the higher-energy STIs are Pd_3: $D_{\infty h}$ linear chain, Pd_4: D_{4h} square and D_{2h} rhombus, Pd_5: $C_{4,v}$ tetragonal pyramid, Pd_6: C_{2v} capped trigonal bipyramid, Pd_7: C_{3v} capped octahedron, C_{3v} tricapped tetrahedron, and Pd_{13}: O_h cuboctahedron.
[20] The thermal accessibility of an *N* atom isomer is estimated by $T = 2(NE_{B,\mathrm{GS}} - NE_{B,\mathrm{isomer}})/(3N - 6)k_B$.
[21] For both the neutral (0.69 eV/atom) and anionic (1.29 eV/atom) dimers the calculated binding energies overestimate somewhat the experimental values of 0.52 ± 0.08 and 1.08 ± 0.09 eV/atom (see Ref. [7]), respectively.
[22] $\langle R_{nn} \rangle$ values range from 2.53 Å (2.49 Å) for Pd_2 (Pd_2^-) to 2.77 Å (2.78 Å) for Pd_{13} (Pd_{13}^-). The reduced bond length of the spin doublet GS of Pd_2^- agrees with experiments (0.037 Å reduction) [8]. Inspection of the KS molecular orbitals (MO) of Pd_2 reveals that the highest occupied MO and the lowest unoccupied one (LUMO) are *both sd* hybridized *bonding* states of the same spatial symmetry but with different spins, and consequently formation of the dimer anion (involving occupation of the LUMO) strengthens the bond and shortens it.
[23] C. Kittel, *Introduction to Solid State Physics* (Wiley, New York, 1996).
[24] V. Spasov and K. Ervin, J. Chem. Phys. **109**, 5344 (1998).
[25] Indeed, the lowest measured [8] electron binding energy peak for Pd_3^- at 1.66 eV essentially coincides with the vDE determined from the PES of Pd_2^- [7] (see open circle for $N = 2$ in Fig. 2b). However, the measured PES peak at 1.66 eV does not exhibit a vibrational structure characteristic to a dimer [8].
[26] J. Ho *et al.,* J. Phys. Chem. **93**, 6987 (1990).
[27] *CRC Handbook of Chemistry and Physics,* edited by R. C. Weast (CRC Press, Cleveland, OH, 1974), 55th ed.
[28] J. F. Janak, Phys. Rev. B **18**, 7165 (1978).
[29] Such an anomalous behavior was observed in SG experiments for large Fe clusters (Ref. [1]) and it has been attributed to a crystal phase transformation, in analogy with the expected coexistence at finite temperature of the D_{5h} and capped O_h structures found here for Pd_7.
[30] U. Heiz and W-D. Schneider, in *Metal Cluster at Surface,* edited by K. H. Meiwes-Broer (Springer, Berlin, 2000).